

ENCLOSURE 3 TO LAP-83-576

NF-1583.02-1

Nonproprietary Version

METHODS OF RECORD  
AN LWR FUEL ASSEMBLY BURNUP CODE  
AMENDMENT 1  
(NONPROPRIETARY VERSION)  
RESPONSE TO NRC QUESTIONS  
DECEMBER 1983

APPROVED BY:

*B. J. Gitnick* 12-22-83  
B. J. Gitnick

Principal Engineer - In-Core Analysis

CAROLINA POWER & LIGHT COMPANY  
411 FAYETTEVILLE STREET MALL  
RALEIGH, NORTH CAROLINA 27602

8401130266 840103  
PDR ADOCK 05000324  
P PDR

(8688WRM/ccc)

## INTRODUCTION

This amendment to Topical Report NF-1583.02, "Methods of RECORD: An LWR Fuel Assembly Burnup Code," is provided in response to requests for additional information as conveyed by Enclosure 1 of the letter to Mr. E. E. Utley, CP&L, from Mr. Domenic B. Vassallo, NRC Division of Licensing, dated November 1, 1983.

QUESTION 1 (NF-1583.02)

(Section 3)

Are thermal spectrum regions user or code defined? The example in Figure 3.0.1 shows pin cells near the control blade to be in the same region with pin cells from the narrow-wide corner of the assembly. If the code made this selection what criterion does it use? What are the maximum number of thermal spectrum regions that may be defined?

RESPONSE

Thermal spectrum regions are either user or code-defined. Through the code input, the user may specify arbitrarily which lattice cells are to be grouped together under one given thermal spectrum region. Up to six such regions may be specified (a dimension limitation only). When not defined in the input, a default criterion in the code selects thermal spectrum regions in accordance with initial U235 enrichment distribution, distinguishing between edge and central lattice positions, and cells in the vicinity of water rod positions. The default option does not distinguish between presence or non-presence of control absorbers in the water gaps; when wanting to take this into account, the input option must be used.

The example in Figure 3.0.1 was generated with the default criterion.

QUESTION 2 (NF-1583.02)

(Section 3.5)

The point energy approach is not described in sufficient detail. In particular more information is needed on the manner in which cross section data are derived from the tabulated 60-180 energy point values in the data library for the determination of the neutron flux at a given energy point value. Similar information is needed with respect to the calculation of the flux disadvantage factors.

RESPONSE

The Point Energy Approach generally improves all numerical integrations which occur during the calculation of thermal energy transfer integrals, thermal reaction rate integrals, etc., in RECORD. (See Appendix A.)

These improvements are obtained by more accurate numerical integration formulas, as well as special treatment of subintegral functions. Thus, about the same accuracy is obtained using 15 "energy (or velocity) points" as with 54 velocity groups in a traditional thermal multigroup scheme (0, 1.84 eV).

Comparisons of results in 15 velocity points with reference multigroup THERMOS results obtained in a 54-group-scheme are provided in Table 2.1.

For each isotope RECORD reads the multigroup (60 or 180 groups) cross-sections from the library. The cross-section values in the 15 velocity points are obtained from the multigroup tables by linear interpolations.

The disadvantage-factor calculations are performed in the same 15 velocity points as mentioned above, using the same "15-point cross-sections."

All calculations in RECORD of thermal neutron spectra and thermal data on a "microgroup level" are performed in the 15 velocity points.

TABLE 2.1 Relative Fuel Absorption Rates

Burnup (MWd/kg)	Isotope	Number of RECORD Energy Points		THERMOS 54 Groups
		15	30	
10	U235	0.485	0.487	0.488
	U238	0.144	0.146	0.145
	Pu239	0.329	0.326	0.326
	Pu240	0.042	0.041	0.041
20	U235	0.307	0.309	0.310
	U238	0.162	0.163	0.163
	Pu239	0.454	0.453	0.452
	Pu240	0.108	0.106	0.105
30	U235	0.180	0.182	0.182
	U238	0.185	0.186	0.187
	Pu239	0.527	0.526	0.526
	Pu240	0.108	0.106	0.105
40	U235	0.093	0.094	0.094
	U238	0.205	0.207	0.207
	Pu239	0.570	0.570	0.570
	Pu240	0.132	0.129	0.129

QUESTION 3 (NF-1583.02)

(Page 3-12)

What is meant by "The rest of the scattering matrix is left almost uncorrected"? Describe the magnitude and basis for any correction.

RESPONSE

"The rest of the scattering matrix is left uncorrected." For further details, and for the numerical effects of the interpolation method, see Appendix A and Table 2.1 of this response.

QUESTION 4 (NF-1583.02)

(Eqs. 3.6.2, 3.6.4, and 3.6.10)

In 3.6.2 the  $N^k$  should be  $\hat{N}^k$ .

In 3.6.4  $F = \bar{\psi}_1 / \psi$  should be  $F = \bar{\psi}_1 / \bar{\psi}$ .

In 3.6.10  $\sigma_s^k$  should be  $\sigma_{tr}^k$  in the equation for  $\Sigma_{tr}^R$ .

RESPONSE

We regret the following typing errors, and confirm that:

In Equation 3.6.2,  $N^k$  should be  $\hat{N}^k$

In Equation 3.6.4,  $F_1 = \bar{\psi}_1 / \psi$  should be  $F_1 = \bar{\psi}_1 / \bar{\psi}$

In Equation 3.6.10,  $\sigma_s^k$  should be  $\sigma_{tr}^k$  in the equation for  $\Sigma_{tr}^R$

QUESTION 5 (NF-1583.02)

(Page 3-15)

Comment on the effect on  $k_{\infty}$  and flux ratios of assuming a macrogroup removal cross section that is constant over a given thermal spectrum region with the use of pin-wise values for all other macrogroup constants.

RESPONSE

The effect on  $k_{\infty}$  and flux ratios of assuming a macrogroup removal cross-section that is constant over a given thermal spectrum region is negligible. Comparison of results from a RECORD run, using 64 spectrum regions, and a run using the default option (6 spectrum regions in an 8x8 assembly) is given in Table 5.1. The deviation in  $k_{\infty}$  between the two runs was 0.00023  $\Delta k$ .



TABLE 5.1 Variation of Flux Ratio Over a Fuel Assembly Diagonal (8 x 8 - BWR, 40% Void), Using 64 Spectrum Regions (Ref.) and 6 Spectrum Regions (Default)

FLUX RATIO I = $\phi_5 / \phi_4$				
Pin Cell Region	Ref.	Default	Default/Ref.	
1				2, 3
10				
19				
28(WR)				
37				
46				
55				
64				

QUESTION 6 (NF-1583.02)

(Eq. 3.6.9)

The definition for the thermal diffusion coefficient in this equation is non-standard. Please comment on its validity, including any assumptions made in its derivation.

RESPONSE

The definition of thermal diffusion coefficient is based on Equation 8.12 in Weinberg & Wigner, "The Physical Theory of Neutron Chain Reactors" (University of Chicago Press, 1958).

$$D = \frac{\Sigma_s}{3\Sigma(\Sigma - \mu\Sigma_s)} \quad , \quad \Sigma = \Sigma_t = \Sigma_a + \Sigma_s$$

When  $\Sigma_a \ll \Sigma$ , this equation reduces to the more usual and standard expression:

$$D = \frac{1}{3\Sigma_s(1 - \mu)} = \frac{1}{3\Sigma_{tr}}$$

QUESTION 7 (NF-1583.02)

(Eqs. 4.1.1 and 4.1.2)

These equations appear to be different from the usual B-1 equations which do not contain a group dependent buckling. Also in the definition of  $h(u)$  a single buckling rather than a group dependent buckling is used. Please comment.

RESPONSE

The buckling terms in Equations 4.1.1 and 4.1.2 are actually independent of energy and should be replaced by constant buckling values, as shown in the definition of  $h(u)$  on Page 4-3. The symbol definition for buckling on Page 4-3 should also be shown as a constant  $B$ , not  $B(u)$ .

QUESTION 8 (NF-1583.02)

(Page 4-4)

Comment on the magnitude of the error made in neglecting inelastic scattering in all isotopes but U-238 in the calculation of the epithermal spectrum and macrogroup constants.

RESPONSE

Inelastic scattering is not neglected. It is taken into account by using a normalized, inelastic scattering matrix for U-238 multiplied by the inelastic scattering cross-sections for each isotope (in each of the 35 epithermal microgroups).

QUESTION 9 (NF-1583.02)

(Eq. 4.2.8)

How is the effective fuel temperature used in this equation obtained? Are spatial effects in the rod and assembly and effects of exposure treated?

RESPONSE

The effective fuel temperature used in Equation 4.2.8 (the effective Doppler temperature) is given in input, and is obtained by the user from engineering correlations, fuel performance codes, etc. Spatial effects in the fuel rod and effects of exposure are not treated in RECORD. However, exposure dependent Doppler corrections are made in PRESTO based on the difference between PRESTO local fuel temperature (power-dependent) and the RECORD reference temperature. See Response to Question 11 (NF-1583.03) in the accompanying document NF-1583.03-1.

QUESTION 10 (NF-1583.02)

(Page 4-11)

What is the basis for determining that a new resonance integral and resonance distribution function are necessary? This implies that data in the library are not interpolated to current conditions. Please comment.

RESPONSE

The resonance integral for U238 is a function of fuel pellet radii and fuel temperature. The resonance distribution functions for U238 are tabulated parametrically in fuel pellet radii and fuel temperature.

For U235, Pu239, Pu240 and Pu241, the resonance integral and resonance distribution functions are tabulated in the Library as functions of fuel pellet radii and enrichment. The resonance distribution functions and resonance integrals are interpolated at each burnup step, according to the corresponding isotopic concentrations, thus following current conditions.

QUESTION 11 (MF-1583.02)

(Page 4-14)

What is the basis for the screening factors used to account for non-uniform lattice effects?

RESPONSE

The screening factors (Dancoff Factors) are based on geometrical considerations for nonuniform lattice effects. A correction factor of  $5/8$  is applied for edge pins to account for 3 out of 8 "missing neighbors." Correspondingly, the correction factor for corner pins is  $3/8$ .

QUESTION 12 (NF-1583.02)

(Section 4.4.2)

Are macrogroup microscopic cross-sections obtained for the epithermal group? If so, how are they obtained? If not, please explain.

RESPONSE

We assume that this question refers to the scattering removal cross-section, (Section 4.4.2). Macrogroup microscopic scattering removal cross-sections are not needed in RECORD. Only the macrogroup macroscopic scattering removal cross-section is needed (and calculated) for generation of the source term in the diffusion equation. The macrogroup microscopic absorption and fission cross-sections are used in the burnup equations, and are obtained according to Eq. 4.4.2.



QUESTION 13 (NF-1583.02)

(Section 5.1)

How is the fuel buffer zone homogenization performed to obtain constants for this region? What modifications are made to account for the presence of an additional gadolinium bearing rod in this zone? How are water rods treated?

RESPONSE

The homogenization of the fuel buffer zone is performed by volumetric averaging, including water rods, if any. The presence of additional gadolinium rods in the buffer zone is not accounted for in the model. This is in agreement with the conclusions of a recently presented NEACRP-report (NEACRP-A-567, 17 Oct 1983).

QUESTION 14 (NF-1583.02)

(Page 5.2)

The use of GADPOL in a geometry identical to that used in RECORD to ensure conservation of the THERMOS generated reaction rates is clear. It is not clear, however, that "any mesh in RECORD may be freely chosen . . . and still get the correct reaction rates and burnup distribution " Please elaborate.

RESPONSE

The sentence on Page 5-2 should be: "Any reasonable mesh in RECORD may then be freely chosen . . . and still get the correct reaction rates and burnup distribution, provided the same mesh point distribution is applied in GADPOL." The point is the GADPOL mesh must match the RECORD mesh, however the RECORD mesh is chosen.

QUESTION 15 (NF-1583.02)

(Page 5-3)

How are the results from the "epithermal group"-in THERMOS transferred to RECORD?

RESPONSE

The results from the "epithermal group" in THERMOS are not transferred to RECORD. Since the depletion of gadolinium is calculated in THERMOS, this artificial "epithermal group" is used in THERMOS to approximately account for the effect of (the small) epithermal absorption in gadolinium on the depletion of Gd-isotopes. The epithermal absorption in Gd is treated explicitly in RECORD using multigroup microscopic cross-sections for Gd-155 and Gd-157, along with approximate number densities (from THERMOS depletion).

QUESTION 16 (NF-1583.02)

(Page 5-3)

Is burnup of fuel isotopes performed in the "buffer" region as well as in the absorber rod? If not, comment on the effect of this neglect.

RESPONSE

Isotopes in the "buffer" region are not depleted in THERMOS. The outer water ring has the major role in maintaining the appropriate thermal spectrum within the poison pin and results are tabulated as functions of the integrated poison pin surface flux. Minor variations in the "buffer" source spectrum have negligible effect on the poison depletion.

QUESTION 17 (NF-1583.02)

(Page 5-4)

It is implied that the treatment of epithermal absorption in shim rods is different from that used for gadolinia rods. Please explain. (See Question 15.)

RESPONSE

The treatment of shim rods is different from the method used for gadolinium. For shim rods the depletion of burnable isotopes ( $B^{10}$ ) is performed in RECORD. Effective thermal microscopic cross-sections are generated with THERMOS/GADPOL, and are given as a function of burnup (or time-integrated surface flux). In this "first" depletion of  $B^{10}$  in THERMOS, an artificial "epithermal group" is applied (as in the gadolinium model).

QUESTION 18 (NF-1583.02)

(Chapter 6)

The control rod formulation used in RECORD has been verified against transport theory calculations performed in the 50's and 60's. Have any comparisons been made to more modern calculations (e.g., Monte-Carlo)?

RESPONSE

The control rod formulations used in RECORD have been verified against published "exact" transport theory numerical solutions for slab absorbers and cylindrical absorbers. These benchmarks are equally valid today. Further numerical verification has not been performed, however, the accumulated experience of many users for many years with rodded conditions in PRESTO provides additional confidence in the model and has not indicated any systematic bias or trend, compared to measured data in operating cores. (See f.ex. the HATCH gamma scan results, NF-1583.03, Chapter 11.3.)

QUESTION 19 (NF-1583.02)

(Section 6.1.2)

Is the RECORD methodology appropriate for the calculation of the proposed General Electric hybrid control rods?

RESPONSE

The control rod methodology in RECORD is equally applicable for Hafnium and  $B_4C$  absorbers and is appropriate for the proposed General Electric hybrid control rod. A new version of RECORD's cross-section library, with data for Hafnium included, is being developed for this application.

QUESTION 20 (NF-1583.02)

(Eq. 7.4.10)

The subscript on the  $j$  index should be  $\tilde{j}-1$  rather than  $\tilde{j},1$ .

RESPONSE

We confirm that, in Equation 7.4.10, the subscript on the  $j$  index should be  $\tilde{j}-1$  rather than  $\tilde{j},1$ .



QUESTION 21 (NF-1583.02)

(Page 8-3)

Quantify the statement that the fission product representation chosen for RECORD showed good agreement with the exact representation for burnup to about 30 GWD/TU. In view of the current trend toward higher burnup fuels should this comparison not be extended?

RESPONSE

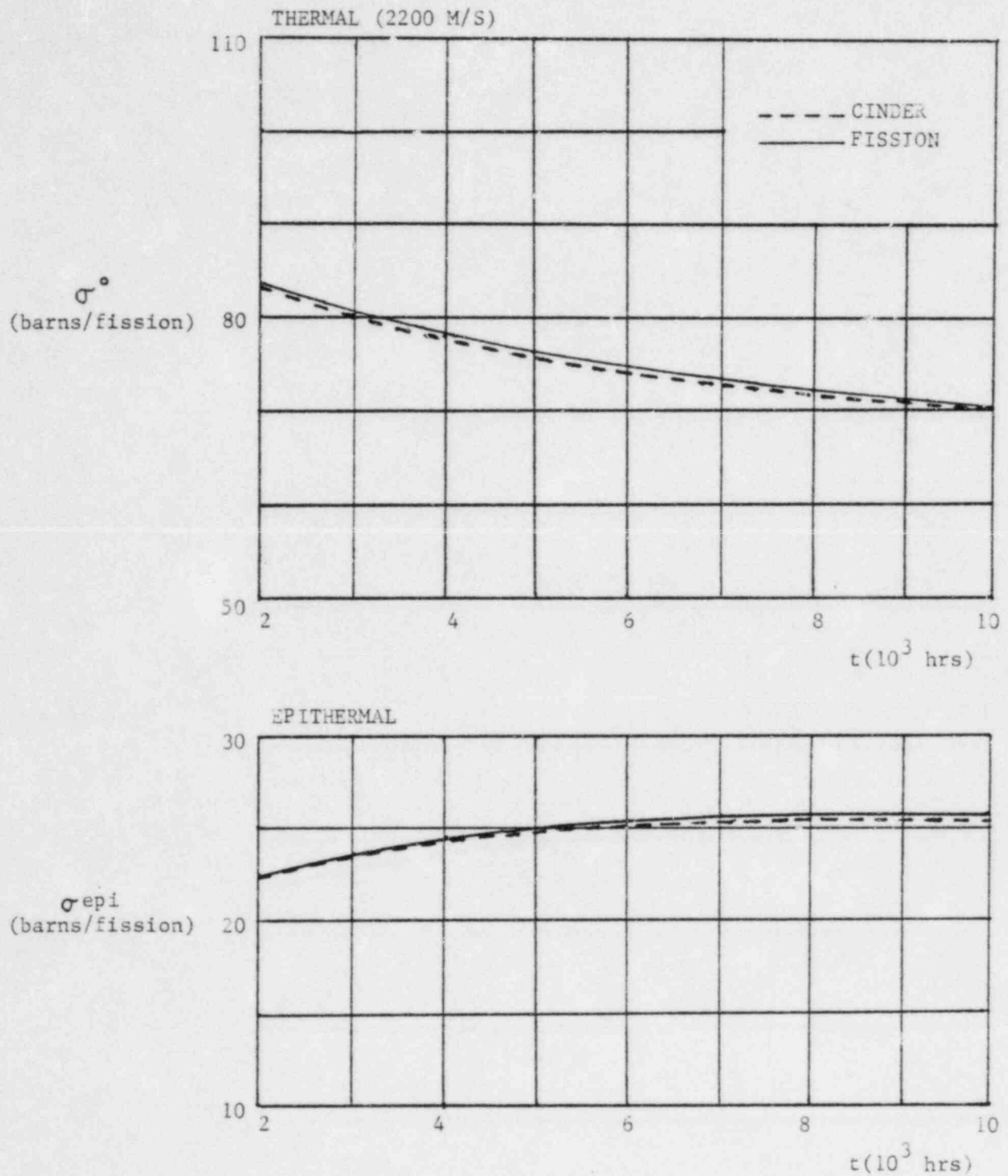
The accuracy of the present fission product model of RECORD is illustrated in Figure 8.2.2 (in NF-1583.02, curves identified by III), in comparison with "exact," explicit solutions (curve I). The agreement in the effective thermal absorption cross-section (barns/fission) is about at 15,000 MWD/TU and at 30,000 MWD/TU for the case considered (BWR, 40% void). Thus, extrapolation beyond 30,000 MWD/TU indicates increasing uncertainty with burnup. However, these model-related uncertainties are generally smaller than those related to basic data.

A revised fission product model with 30 explicit isotopes is now being developed for RECORD for high burnup PWR analysis. This new model is expected to yield improved agreement with the fully explicit reference model, both at intermediate and high burnup ( $> 30,000$  MWD/TU). Once the modifications are complete, a study will be performed to determine the adequacy of the present model for high burnup BWR fuel.

A comparison of the reference model with CINDER results is shown in Figure 21.1.

2, 3

FIGURE 21-1



QUESTION 22 (NF-1583.02)

(Section 9.1)

Please provide a discussion of the treatment of LPRM's or verify that it is the same as that used for the TIP.

RESPONSE

The treatment of LPRM's, from a RECORD point-of-view, is the same as that used for TIP's.

QUESTION 23 (NF-1583.02)

(Section 9.1)

Is the correlation for the effective U-235 cross-section based on data from various burnups, rod configuration, etc.? If not, provide a discussion of such effects on the U-235 cross-section.

RESPONSE

The correlation for default U-235 cross-sections for the TIP model in RECORD is based on data for various fuel types and in-channel average voids. The spectral effects of fuel burnup, rod configuration, self-shielding, etc., are secondary to the void effect as is shown by the TIP comparisons summarized in Tables 5.5.1 and 5.5.2 of NF-1583.01 and the figures given in Amendment 1 (NF-1583.01-1) in response to Question 11. The standard deviation of nodal measured-calculated differences was 8.9% of which the measurement component is attributed to be 6.7%.

QUESTION 24 (NF-1583.02)

(Section 9.2)

Typos

Eq. 9.2.1  $B_{\text{eff}}^i$ ,  $\lambda$  instead of  $B_{\text{eff}}^i$ ,

Eq. 9.2.4  $a_{\lambda}^i$  instead of  $a_{\lambda}$ ,

Eq. 9.2.8 (Denom)  $a_{\lambda}^i$  instead of  $a^i$

RESPONSE

We regret the following typing errors, and confirm that:

In Equation 9.2.1,  $\beta_{\text{eff}}^i$ , should be  $\beta_{\text{eff}}^i$ ,  $\lambda$

In Equation 9.2.4,  $a_{\lambda}$  should be  $a_{\lambda}^i$

In Equation 9.2.8,  $a^i$  should be  $a_{\lambda}^i$

QUESTION 25 (NF-1583.02)

(Chapter 10)

The comparisons between RECORD and experimental values of k-effective for  $\text{UO}_2$  and  $\text{PuO}_2$  lattices used the calculated (by MD-1) values of buckling. How did these bucklings compare with the measured buckling values for those experiments that had measured values?

RESPONSE

It should be made clear that in the Scandpower analyses of the clean critical lattices, measured buckling values were applied in both RECORD and MD1.

The 5-group data for the lattice regions were generated with RECORD in single-pin option, using the measured total buckling in the leakage calculation. However, for a small configuration where the leakage is relatively high, this simple treatment of leakage in RECORD gives significant uncertainty. In order to obtain a more adequate validity check of the lattice data generated by RECORD, one-dimensional diffusion calculations were performed in cylindrical geometry representative of the actual lattices, using the MD1 code. A cylindrical homogeneous core model was used with an equivalent radius obtained from the experimental configuration together with an outer homogeneous reflector. The axial leakage was represented by the measured axial buckling. As the axial leakage is much less than the radial leakage for these lattices, this gives more correct  $k_{\text{eff}}$  values.

The deviations of resulting  $k_{\text{eff}}$  values from unity are interpreted as measures of the accuracy of the codes for the analysis.

QUESTION 26 (NF-1583.02)

(Chapter 10)

Have comparisons been made to measured quantities such as  $\rho_{28}$  and  $\delta_{25}$  for critical experiments (TRX experiments, for example)? If so, what were the results?

RESPONSE

The reaction rate parameters,  $\rho_{28}$  and  $\delta_{25}$ , are defined as:

$\rho_{28}$  = non-thermal captures in U238 per thermal capture in U238

$\delta_{25}$  = non-thermal fissions in U235 per thermal fission in U235

where both  $\delta_{25}$  and  $\rho_{28}$  are related to the cadmium cut-off at about 0.4 eV.

Table 26.1 provides results of calculations performed by Scandpower using the code CRISP in comparison with experimental data (Refs. 27, 49, and 50). This code was the predecessor of RECORD, corresponding to RECORD in a single-pin mode.



TABLE 26.1 Comparison of Theoretical and Experimental  $\delta_{25}$  and  $\rho_{28}$ 

CASE	$\delta_{25}$		$\rho_{28}$	
	CRISP	EXP.	CRISP	EXP.
ND1	0.020		0.356	0.374
ND2	0.042		0.778	
ND3	0.075		1.369	1.292
ND4	0.140		2.558	2.205
ND5	0.180		3.265	2.893
BN1	0.183		3.288	2.92±0.09
BN2	0.148		2.669	2.41±0.04
BN3	0.116		2.105	1.81±0.06
BN4	0.086		1.576	1.41±0.02
BN5	0.063		1.159	1.04±0.02
W9	0.088	0.089±0.002	1.454	1.43±0.01
W10	0.072	0.072±0.001	1.209	1.15±0.01
W11	0.055	0.055±0.001	0.942	0.934±0.01
BN-U1	0.217		2.647	2.44±0.1
BN-U2	0.142		1.764	1.61±0.1
BN-U3	0.106		1.338	1.35±0.06
BN-U4	0.072		0.921	0.93±0.03
BN-U5	0.056		0.716	0.73±0.03
BN-U6	0.251	0.261	2.962	
BN-U7	0.163	0.183	1.933	1.80±0.18
BN-U8	0.122	0.132	1.449	1.24±0.12
BN-U9	0.084	0.066	0.988	0.89±0.09
BN-U10	0.065	0.050	0.768	



QUESTION 27 (NF-1583.02)

(Table 10.4.1)

Comment on the poor agreement for Maine Yankee, Cycle 1.

RESPONSE

The Maine Yankee, Cycle 1, results were obtained with preliminary PWR versions of RECORD/PRES10 as part of a development effort. The poor agreement in  $k_{eff}$  is probably caused by rough modeling of the shim rods and a model for the moderator boron concentration which has since been improved.

QUESTION 28 (NF-1583.02)

(Figures 10.2.1-10.2.8)

These figures appear to be mislabeled. Those were Yankee Rowe - not Maine Yankee - experiments were they not?

RESPONSE

We regret the mistake in Figures 10.2.1 to 10.2.8. The Figures refer, of course, to Yankee Rowe experiments and not to Maine Yankee, as is clear from the text in Section 12.

THE POINT ENERGY METHODOriginal Reference

Below we will give some comments to the "Point Energy Approach" and also show some comparisons of results obtained using 15 velocity points with reference THERMOS results obtained in a 54-group-scheme.

In RECORD, the reaction rate integral:

$$R = \int_0^{v^*} \Sigma(v) v N(v) dv$$

is calculated by dividing the interval  $(0, v^*)$  into  $N$  subintervals where, in each of them, the subintegral function is easier to integrate. A Gaussian integration scheme is applied on a transformed integrand, using variable transformation which condenses the Gaussian points toward the range of a resonance influence.

Having  $N$  above mentioned subintervals, and a substitution function  $v = \phi_n(t)$ , we have:

$$\int_0^{v^*} f(v) dv = \sum_{n=1}^N \int_{t_{n0}}^{t_{n1}} f(\phi_n(t)) \frac{d\phi_n}{dt} dt$$

Using further substitution which reduces each interval of integration to the interval  $(0,1)$ , and using  $R_n$ -points Gaussian formula in each subinterval, one obtains

$$\int_0^{v^*} f(v) dv = \sum_{n=1}^N \sum_{r=1}^{R_n} w_r f\left\{\phi_n[(t_{n1} - t_{n0})x_r + t_{n0}]\right\} \frac{d\phi_n}{dt} \bigg|_{t=v_r} (t_{n1} - t_{n0})$$

where  $x_r$  and  $w_r$  are Gaussian points and weight coefficients, respectively, (both for interval  $(0,1)$ ). The following relations for modified Gaussian points and weight coefficients are used:

$$v_i = \phi_n [(t_{n1} - t_{n0})x_r + t_{n0}]$$

$$w_i = \phi_n [(t_{n1} - t_{n0}) \sum_{\ell=1}^r w_\ell + t_{n0}] - \phi_n [(t_{n1} - t_{n0}) \sum_{\ell=1}^{r-1} w_\ell + t_{n0}]$$

where

$$i=1,2,\dots,K, n=1,2,\dots,N, r=1,2,\dots,R_n, K = \sum_{n=1}^N R_n$$

and we can write

$$\int_0^{v^*} f(v) dv = \sum_{i=1}^K W_i f(v_i)$$

The substitution functions,  $v = \phi(t)$ , were emphasized to approximate, very roughly at best, the inverse function of the integrand. The modified weight coefficients were defined under the assumption that the transformed integration point is an approximation of the original integrand mean value over the interval corresponding to the respective Gaussian weight coefficients.

The variable transformations  $v = \phi(t)$ , which were used in each of the subintervals, are listed in the following Table A-1:

Table A-1 Subintervals and Variable Transformations ( $\Gamma = 0.1$  eV)

Sub-interval	Upper limit	Variable transformation
I		
II		
III		
IV		
V		
VI		

2,3

The energy transfer integral, which appears in the transport equation, is either in group or discrete velocity representation, approximated by a numerical integration formula:

$$I = \int_0^{v^*} G(v' \rightarrow v_j) N(v') dv' = \sum_{i=1}^K W_i G_{ij} N_i$$

In order to improve the accuracy of this approximation, the behavior of the scattering kernel and the neutron spectrum in the vicinity of point  $i$  have been taken into account. Splitting the integral into a sum of integrals over the intervals.

$$\langle v_{di} = \sum_{\ell=1}^{i-1} W_{\ell ij}; v_{ui} = \sum_{\ell=1}^i W_{\ell} \rangle$$

$$I = \sum_{i=1}^K \int_{v_{di}}^{v_{ui}} G(v' \rightarrow v_j) \frac{N(v') dv'}{v_j}$$

Assuming the point values of the neutron spectrum to be known, we can express the velocity dependence of the spectrum in the vicinity of point  $i$  by the LaGrange interpolation formula, taking into account the spectrum values in  $2M$  additional nearest points:

$$N(v) = \sum_{k=k_{\min}}^{k_{\max}} N_k L_k^i(v)$$

where

$$k_{\min} = \max(1, i-M) \quad k_{\max} = \min(K, i+M)$$

and we assume:

$$N(v) \sim v^2 \text{ for } v < v_i$$

and

$$N(v) \sim 1/v^2 \text{ for } v > v_k$$

We obtain:

$$G_{ij} = \sum_{k=k_{\min}}^{k_{\max}} \frac{1}{W_i} \int_{v_{dk}}^{v_{uk}} dv' G(v' \rightarrow v_j) L_k^i(v')/v_j$$

Using R-point Gaussian integration formula, we have

$$G_{ij} = \sum_{k=k_{\min}}^{k_{\max}} \frac{W_k}{W_i} \sum_{r=1}^R \frac{w_r}{v_j} G[v'(v_r) \rightarrow v_j] L_k^i v'(v_r)$$

where

$$v'(v_r) = W_k \cdot v_r + \sum_{\ell=1}^{k-1} W_{\ell}$$

and where  $v_r$  and  $w_r$  are Gaussian points and weight coefficients for the interval  $(0,1)$ . In RECORD, we use an integration scheme with  $M=0$ ,  $R=4$  for  $i=j$  only.

The source term  $S(v)/v$  in the transport equation may also be corrected in a simple way. The total neutron source into the thermal energy interval is calculated by

$$\int_0^{v^*} \frac{S(v)}{v} dv = \sum_{i=1}^K \int_{a_i}^{b_i} \frac{\sum_{se} \frac{1}{1-\alpha^2} \left( \frac{1}{v^{*2}} - \frac{\alpha^2}{v^2} \right) dv}$$

where

$$a_i = \sum_{\ell=1}^{i-1} W_{\ell} \quad b_i = \sum_{\ell=1}^i W_{\ell}$$

we obtain:

$$S_i = \begin{cases} \frac{\sum_{se} v_i}{1 - \alpha^2} \left( \frac{1}{v^{*2}} - \frac{\alpha^2}{a \cdot b} \right) & av^* \leq a \leq b \leq v^* \\ \frac{\sum_{se} v_i}{1 - \alpha^2} \left( \frac{1}{v^{*2}} - \frac{\alpha^2}{v^* \cdot b} \right) & a \leq av^* \leq b \leq v^* \\ 0 & a \leq b \leq av^* \end{cases}$$

The applicability of such a method in RECORD was very much dependent on the possibility for obtaining required accuracy with a reduced number of velocity points. A comparison of a calculated thermal neutron spectrum in a homogenized BWR fuel pin cell, using different numbers of velocity points at zero and 40,000 MWD/TU, is shown in Figures A-1 and A-2.

A corresponding comparison of calculated thermal absorption rates is given in Table 2-1 (with Question 2 of this response).

Our conclusion is that application of 15 energy (or velocity) points in RECORD, using the "Point Energy Approach", gives the required accuracy.

Figure A-1

THERMAL NEUTRON SPECTRUM UP TO 2.0 eV

Homogenized BWR single pin cell 0 MWD/T

o 15 point velocity representation

— 30 point (identical with 54 group THERMOS spectrum)

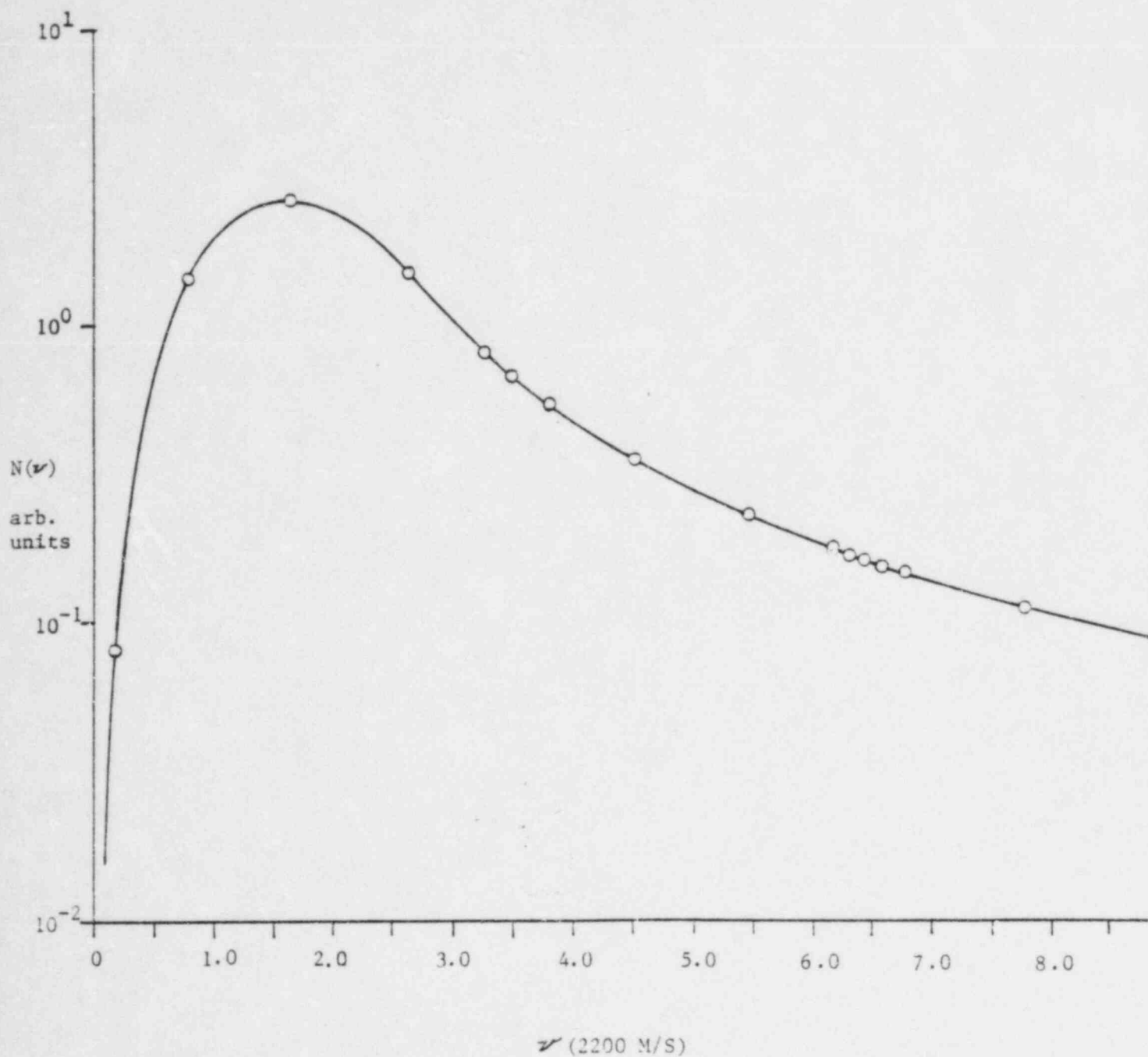




Figure A-2

THERMAL NEUTRON SPECTRUM UP TO 2.0 eV

Homogenized BWR single pin cell 40,000 MWD/T

○ 15 point velocity representation

— 30 point (identical with 54 group THERMOS spectrum)

